Effect of Thermal Treatment on the Electronic Conductivity Properties of Cobalt Spinel Phases Synthesized by Electro-Oxidation in Ternary Alkaline Electrolyte (KOH, LiOH, NaOH)

Myriam Douin,[†,‡,§] Liliane Guerlou-Demourgues,*[,†,‡] Michel Ménétrier,[†,‡] Emilie Bekaert,[†,‡] Lionel Goubault,[§] Patrick Bernard,[§] and Claude Delmas[†,‡]

CNRS, ICMCB, 87, Avenue Dr. A. Schweitzer, 33608 Pessac Cedex, France, Université de Bordeaux, ICMCB, ENSCPB, F33608 Pessac Cedex, France, and SAFT−Direction de la Recherche, 111-113 Boulevard Alfred Daney, 33074 Bordeaux Cedex, France

Received June 30, 2008. Revised Manuscript Received August 29, 2008

A thermal treatment of Co_3O_4 type spinel phases, synthesized by electrooxidation of CoO powder in a mixed alkaline electrolyte (KOH, LiOH, NaOH), is shown to have an important influence on the electronic conductivity properties of the materials. The initial spinel phase contains hydrogen, lithium, cobalt vacancies, and especially Co^{4+} ions within the structure, leading to an electronic conductivity significantly larger than that of stoichiometric Co_3O_4. The thermal treatment, followed by in situ X-ray diffraction, TGA-MS and electronic conductivity measurements, induces a water release, coupled with an increase of the Co/O atomic ratio and a structural reorganization. The resulting cationic redistribution within the spinel framework entails an increase of the Co^{4+} amount in the $[Co_2O_4]$ network and therefore of the electronic conductivity (by 3 orders of magnitude).

Introduction

Co_3O_4 was investigated in a diversity of fields. It is, from the application point of view, an important material, studied with regard to magnetic,[1,2] catalytic,[3] and gas sensing properties,[4,5] but also as negative electrode material in lithium batteries.[6,7] Recently, a "Co_3O_4" derivative, which can be used as electronic conductive additive in the positive electrode of alkaline batteries, was studied in our laboratory.[8,9]

The structure of ideal cubic Co_3O_4, which is a normal spinel with the general formula AB_2O_4, can be described as a $[Co_2O_4]$ framework of Co^{3+} ions in edge-sharing octahedral B sites, where Co^{2+} ions are located in tetrahedral A sites that share only corners with the octahedra. An overlapping of the cobalt t_{2g} orbitals across the shared edges of the CoO_6 octahedra occurs. In the case of ideal Co_3O_4, the t_{2g} band is completely filled because of the electronic configuration of Co^{3+} (d^6 LS) ions, leading to a semiconductor behavior with a very low electronic conductivity. As reported in the literature, a p-type metallic conductivity can be achieved, if a cobalt mixed valency (Co^{3+}/Co^{4+}) exists in the octahedral sublattice and entails electronic delocalization.[10−12] Such a behavior can be obtained by partial substitution of Li^+ ions for cobalt ones, which involves the presence of Co^{4+} ions in the octahedral B sites for charge compensation. Lithiated cobalt oxide spinel phases can be prepared by solid state reaction,[10,12−14] or by soft chemistry reaction such as thermal decomposition[11] or reaction with *n*-butyl lithium.[6] Depending on the method, lithium ions may occupy cobalt sites (tetrahedral 8a, octahedral 16d) and/or vacant sites (tetrahedral 8b, octahedral 16c) in the spinel lattice.

In our laboratory, we focused on battery-related H_xLi_y-$Co_{3-\delta}O_4$ spinel type materials, exhibiting a high electronic conductivity; they were synthesized, via an electrochemical oxidation original method, starting from CoO.[8] Such phases were shown to contain cobalt vacancies in both tetrahedral and octahedral sites, and lithium and hydrogen in the structure. The negative charge resulting from cobalt vacancies is only partially compensated by lithium and hydrogen, thus resulting in the formation of Co^{4+} ions in the octahedral sites and in an increase of conductivity versus ideal Co_3O_4. The presence of hydrogen in the structure, which is likely to be removed at high temperature, leads to the following question:

* Corresponding author. E-mail: guerlou@icmcb-bordeaux.cnrs.fr.
† CNRS, ICMCB.
‡ Université de Bordeaux,.
§ SAFT−Direction de la Recherche.

(1) Ichiyanagi, Y.; Kimishima, Y.; Yamada, S. *J. Magn. Magn. Mater.* **2004**, *272−276* (Supplement 1), E1245–E1246.
(2) Makhlouf, S. A. *J. Magn. Magn. Mater.* **2002**, *246* (1−2), 184–190.
(3) Smith, W. L.; Hobson, A. D. *Acta Crystallogr., Sect. B* **1973**, *29*, 362.
(4) Wöllenstein, J.; Burgmairb, M.; Pleschera, G.; Sulimab, T.; Hildenbranda, J.; Böttnera, H.; Eiseleb, I. *Sens. Actuators, B* **2003**, *93* (1−3), 442–448.
(5) Li, W. Y.; Xu, L. N.; Chen, J. *Adv. Funct. Mater.* **2005**, *15* (5), 851.
(6) Thackeray, M. M.; Baker, S. D.; Adendorff, K. T.; Goodenough, J. B. *Solid State Ionics* **1985**, *17*, 175.
(7) Larcher, D.; Sudant, G.; Leriche, J.-B.; Chabre, Y.; Tarascon, J.-M. *J. Electrochem. Soc.* **2002**, *149* (3), A234–A241.
(8) Tronel, F.; Guerlou-Demourgues, L.; Ménétrier, M.; Croguennec, L.; Goubault, L.; Bernard, P.; Delmas, C. *Chem. Mater.* **2006**, *18* (25), 5840–5851.
(9) Bernard, P.; Goubault, L.; Delmas, C.; Tronel, F.; Guerlou-Demourgues, L.; Shaju, K. M. Patent FR 2 884 355, 2006.
(10) Appandairan, N. K.; Viswanathan, B.; Gopalakrishnan, J. *J. Solid State Chem.* **1981**, *40*, 117.
(11) Zhecheva, E.; Stoyanova, R. *Mater. Res. Bull.* **1991**, *26*, 1315.
(12) Zhecheva, E.; Stoyanova, R.; Angelov, S. *Mater. Chem. Phys.* **1990**, *25*, 351.
(13) Rasiyah, P.; Tseung, A. C. C. *J. Electrochem. Soc.* **1983**, *130*, 365–368.
(14) Antolini, E. *Mater. Res. Bull.* **1997**, *32* (1), 9–14.

10.1021/cm801775g CCC: $40.75
Published on Web 10/11/2008

what is the effect of heat treatment on the structure, composition, and electronic conductivity properties of this material?

Experimental Section

Material Preparation. The material was obtained by electrochemical oxidation of a cobalt-based electrode. The electrode was made from a viscous paste, prepared by mixing CoO powder with 50 wt % deionized water, which was introduced into a porous nickel metallic foam. After drying for 2 h at 85 °C, the foam was pressed at 1 t/cm^2. No mechanical binder, like PTFE, was used, to make the recovery of the material afterward easier. The electrode was placed between two cadmium electrodes, playing both roles of counter and reference electrode, with a polyamide separator intercalated to avoid a short circuit. The cell was then immersed into a ternary concentrated alkaline electrolyte consisting of NaOH, LiOH and majority KOH. In the so-constituted cell, the CoO-based electrode was the positive pole and the Cd-based electrode the negative one. Therefore, charge and discharge of the cell correspond to cobalt oxidation and reduction respectively. The cell was first left during 4 days in the electrolyte in order to allow complete hydrolysis of CoO into $Co(OH)_2$. The electrochemical process then consisted in charging the cell at the *C*/100 rate for 120 h. (The theoretical capacity "*C*" of the battery was calculated on the basis of one electron exchanged per cobalt atom.) Lastly, the positive electrode was rinsed with deionized water to remove any trace of electrolyte, and dried for 15 h at 60 °C. To recover the cobalt material, the electrode was milled and then sieved with an 80 μm mesh, to completely eliminate nickel foam particles. The so-obtained material will be denoted as spinel-start (for starting material) in the following.

Sample Heat-Treatment. The starting material was subjected to a heat-treatment at three interesting temperatures (100, 370, and 650 °C), which were determined on the basis of thermal analysis, reported in the thermal analysis section. These temperatures are indeed located just after peaks in mass loss derivative curves. It should be noted that the temperature 370 °C was chosen just after the top of the peak, because we wanted to avoid the presence of the parasitic $LiCoO_2$ phase, which is likely to be formed around 400 °C. The treatment was carried out with argon, the temperature was increased at the rate of 2 °C/min, followed by an isothermal stage at the target temperature for 4 h. The samples were then cooled in air at ambient temperature, without any special care with regard to hydration. The samples thus obtained at the three temperatures will be denoted as spinel-100, spinel-370, and spinel-650 in the following.

Characterization. Materials were characterized either by ex-situ analysis or in situ analysis. Ex situ analysis consisted in studying the four samples spinel-start, spinel-100, spinel-370, and spinel-650 by X-ray and neutron diffraction, ^{7}Li NMR, TGA, and elementary analysis. In situ analysis consisted of studying spinel-start sample by coupling heat-treatment in air with X-ray diffraction analysis.

X-ray diffraction (XRD) data were collected with a PANalytical X'pert Pro diffractometer using the Co Kα radiation. The diffraction patterns were recorded in the [5−110]° (2θ) angular range, using a 0.0167° (2θ) step, with an active width of 2.122° (2θ) in the detector and a constant counting time of 250 s per step.

To carry out in situ analysis, we coupled X-ray diffraction analysis with heat-treatment. For this purpose, an Anton Paar HTK 1200 high-temperature furnace was connected to the diffractometer. The sample was heated at the rate of 3 °C/min. Isothermal stages of 4 h were programmed at room temperature and then every 100 °C until 600 °C and finally at 650 °C during which the X-ray diffraction data were collected.

Structure refinements were based on the Rietveld method using the Fullprof program.[15] The diffraction peaks were described by a pseudo-Voigt fitting function, in which the Lorentzien contribution to the Gaussian peak-shape was refined. The angular dependence of the widths was expressed by $H^2 = U \tan^2 \theta + V \tan \theta + W$, where H is the full width at half-maximum, θ is the Bragg angle, and U, V, and W are refined parameters. Because of the Co radiation, anomalous scattering factors were added as below: $f'(O) = 0.063$, $f''(O) = 0.044$, $f'(Co) = -2.023$, and $f''(Co) = 0.5731$. Background intensities were fixed with about twenty experimental points. The spinel-type phase was described in the cubic space group $Fd3m$, with oxygen in the 32e position (u, u, u), and cobalt ions located in the 8a tetrahedral sites (1/8, 1/8, 1/8) and in the 16d octahedral sites (1/2, 1/2, 1/2). Scale factor, lattice parameter, atomic position of oxygen, cobalt occupancy, and thermal displacement parameters B were refined. The $LiCoO_2$ type phase that appears in some experiments was described in the $R\bar{3}m$ space group, with oxygen in the 6c position (0, 0, z), cobalt ions in 3a sites (0, 0, 0) and lithium ions in 3b sites (0, 0, 1/2). For this secondary phase, only the scale factor, the lattice parameter, and the oxygen atomic position were refined. Because of the small amount of $LiCoO_2$ phase, its parameters of pseudo-Voigt function were constrained to be the same as those obtained for the spinel phase.

Neutron diffraction data were collected at Institut Laue Langevin in Grenoble (France), on the high-resolution D2B diffractometer, at room temperature, with a scan step of 0.05 ° (2θ) between 0 and 160°. The samples were contained in a vanadium cylindrical sample holder, with a diameter of 8 mm and a height of 5 cm. As for X-ray, the refinement of the neutron data was performed with the Fullprof program. Absorption effects were corrected by using a calculated value of μR equal to 0.381.

^{7}Li MAS NMR spectra were recorded on a Bruker Avance 300 (116.6 MHz) spectrometer, using a standard 2.5 mm Bruker MAS probe with a 30 kHz spinning speed. A single pulse sequence was used with a 90° pulse duration of 2 μs. The recycling time between two scans was 60 s. Spectra are referred to 1 M aqueous solution of LiCl, set at 0 ppm. T1 relaxation times were estimated by using variable recycling times, until full intensity of the line is observed. Decomposition of spectra was achieved using the DMfit software.[16]

Thermogravimetric analysis (TGA) was carried out with a TA Instruments SDT 600 analyzer, under an argon flux, from room temperature to 1000 °C, at a heating rate of 3 °C/min.

Inductively coupled plasma (ICP) was used for Li, Na, K, and Co titrations and elementary organic microanalysis was used for H titration. Titrations were performed at CNRS facility in Vernaison (France). The oxidation state of cobalt was established by iodometric titration method.[8]

Temperature-dependent electronic conductivity measurements were carried out with the four-probe technique,[17] using a direct current. The temperature was decreased to −100 °C, progressively raised to 400 °C, and then lowered to room temperature. Because of the low-temperature synthesis, the studied material could not be sintered. For this reason, pellets (8 mm of diameter and approximately 1.2 mm in thickness) were only obtained by compacting 200 mg of powder at 8 t/cm^2 under a vacuum.

(15) Rodriguez-Carvajal, R. *Satellite Meeting on Powder Diffraction of the XV Congress of the IUCr*, Toulouse, France, July 16−18, 1990; International Union of Crystallography: Chester, U.K., 1990; p 127.
(16) Massiot, D.; Fayon, F.; Capron, M.; King, I.; Le Calve, S.; Alonso, B.; Durand, J.-O.; Bujoli, B.; Gan, Z.; Hoatson, G. *Magn. Reson. Chem.* **2002**, *40* (1), 70–76.
(17) Laplume, J. *L'onde électrique* **1955**, *335*, 113–125.

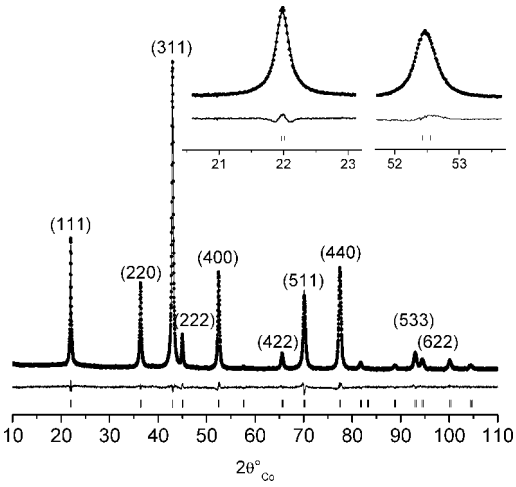

Figure 1. Comparison of the experimental (•) and calculated (−) X-ray powder diffraction patterns of the spinel-start material. The difference between observed and calculated profiles, and the diffraction lines positions (|) of the Co_3O_4 phase are given. The zoom on the (111) and (400) lines, proposed in the inset, allows us to show the good quality of the refinement.

Table 1. Parameters and Reliability Factors, Obtained by Rietveld refinement of the X-ray Diffraction Pattern of the Spinel-Start Material

Spinel ≪Co_3O_4≫ Type Phase, *Fd3m*, $a_{cub.}$ = 8.0824(7) Å						
atom	site	*x/a*	*y/b*	*z/c*	occupancy	*B* (Å)
Co	8a	0.125	0.125	0.125	0.77(2)	0.8(2)
Co	16d	0.5	0.5	0.5	0.96(2)	0.41(9)
O	32e	0.2619(5)	0.2619(5)	0.2619(5)	1.00	0.3(3)
profile parameters						
pseudo-Voigt function	η = 1.00(2)	U = 0.02(4)	V = 0.15(4)	W = 0.036(9)		
reliability factors with Bragg contribution						
R_{cp} = 12.0		R_B = 5.02%				
R_{cwp} = 7.99		χ^2 = 3.66%				

Results

X-ray and Neutron Diffraction Ex Situ Analysis. The X-ray diffraction diagram of the starting material, displayed in Figure 1, is characteristic of a spinel type structure. The results of the refinement are presented in details in Table 1. The pattern can be indexed in the *Fd3m* space group. Oxygen ions, in 32e sites, form a cubic close-packed arrangement, where Co^{2+} ions occupy the 8a tetrahedral sites and Co^{3+} and Co^{4+} the 16d octahedral ones.

Refinements were performed for X-ray and neutron diffraction data, collected for the spinel-100, spinel-370, and spinel-650 heat treated samples. The results are reported in Table 2. They put emphasis on: (i) a decrease, followed by an increase in the spinel cell parameter when heat-treatment temperature increases, (ii) a slight increase of the "*u*" oxygen position parameter, (iii) an increase of cobalt occupancy in tetrahedral sites (8a), whereas the cobalt occupancy in octahedral sites (16d) remains almost stable. Figure 2 displays, as an illustration, the experimental and calculated X-ray diffraction patterns of the spinel-650 sample. The diagram shows the existence of a biphasic material, containing a Co_3O_4 type phase and about 7 wt % of a $LiCoO_2$ type phase (from Rietveld refinement). The appearance of $LiCoO_2$ during thermal treatment is in accordance with the presence of lithium atoms in the initial spinel structure, as confirmed by the NMR characterization reported in this paper. This phase appears to be a HT-$LiCoO_2$ phase, exhibiting an O3 type oxygen packing, with hexagonal cell parameters $a_{hex.}$ = 2.8202(6) Å and c_{hex} = 14.058(4) Å. The formation of such a phase is in agreement with works reported by Thackeray or Antolini, who had observed the formation of a layered $LiCoO_2$ phase, from extensively lithiated Co_3O_4 samples that were heat-treated at 400 °C.[6,14]

To detail the evolutions of the three parameters previously pointed out, the effects of temperature on the material structure were investigated by in situ XRD analysis.

X-ray Diffraction in Situ Analysis. The structural evolution of the Co_3O_4 starting sample during heat treatment was followed by X-ray diffraction, thanks to a variable temperature chamber. For this purpose, after a first data acquisition at room temperature (noted RT-i), the temperature of the chamber was gradually increased to 650 °C, as described in the Experimental Section. X-ray data acquisition was performed at every isothermal stage. To finish, the chamber was cooled to room temperature and a final X-ray diagram (noted RT-f) was recorded. The evolution of the X-ray patterns with temperature is presented in Figure 3. The following modifications can be underlined:

The width of the diffraction lines tends to be reduced, which highlights an improved crystallization of the material.

A general shift of the diffraction lines toward the low angles can be assigned to an increase in the cubic cell parameter, because of thermal dilatation.

The inversion of the (111)/(220) peak intensity ratio suggests a modification of occupancy of cobalt sites, as demonstrated by Tronel et al. thanks to simulation.[8]

Beyond 500 °C, new diffraction lines, assigned to a $LiCoO_2$-type phase, emerge.

Diffraction data refinements were performed with the Rietveld method to clarify these evolutions. The results are reported in Table 3. The observed tendencies confirm and complete those deduced from ex situ analysis of "spinel-start" and of the heat-treated samples. More precisely, the cobalt occupancies in the spinel-start material obtained by ex situ experiment and in the material at the initial RT temperature at the very beginning of the in situ experiment are as expected identical (0.77 for the 8a site and 0.96 for the 16d site, as reported in Tables 1 and 3). The cobalt occupancies in the spinel-100 material obtained by ex situ experiment (0.78 for the 8a site and 0.96 for the 16d site, as reported in Table 2) and in the material obtained at 100 °C during the in situ experiment (0.81 for the 8a site and 0.98 for the 16d site, as reported in Table 3) are close to each other. The cobalt occupancies in the spinel-370 material obtained by ex situ experiment are in full accordance with the values obtained for the in situ materials obtained at 300 °C (0.79 for the 8a site, and 0.98 for the 16d site, as reported in Tables 2 and 3). The cobalt occupancies in the in situ materials obtained at 650 °C and just after cooling to room temperature are quite identical (0.95 against 0.96 for the 8a site and 0.98 against 0.99 for the 16d site, as reported in

Table 2. Comparison of the Rietveld Refinement Structural Parameters (X-ray diffraction and neutron patterns) of the Spinel-100, Spinel-370 and Spinel-650 Heat-Treated Samples

	spinel-100		spinel-370		spinel-650	
	X-ray	neutron	X-ray	neutron	X-ray	neutron
			Spinel ≪Co_3O_4≫ Type Phase, *Fd*3*m*			
$a_{cub.}$ (Å)	8.0796(3)	8.0798(4)	8.0650(4)	8.0645(4)	8.0811(4)	8.0803(3)
oxygen position	0.2621(3)	0.2628(2)	0.2624(3)	0.2632(2)	0.2638(3)	0.2637(2)
Co occupancy (8a sites)	0.78(2)	0.81(7)	0.79(2)	0.74(5)	0.92(2)	0.99(5)
Co occupancy (16d sites)	0.96(2)	1.01(4)	0.98(2)	0.97(3)	0.96(2)	1.00(3)
			$LiCoO_2$ Phase, $R\bar{3}m$			
$a_{hex.}$ (Å)					2.8202(6)	2.820(2)
$c_{hex.}$ (Å)					14.058(4)	14.03(2)
wt %					6.7(3)	5.7(6)

Table 3), which suggests no change within the material during the cooling step. Moreover, these values at the final room temperature for the in situ experiment are also in good accordance with those obtained for the spinel-650 ex situ material (0.92 for the 8a site and 0.96 for the 16d site, as reported in Table 2).

Figure 4a presents the evolution of the $a_{cub.}$ cell parameter as a function of data collection temperature. The values, obtained for the annealed materials, cooled down at room temperature, are also reported (□). The curve shows a slight decrease of the cubic cell parameter until 200 °C, followed by an increase. In first approximation, an increase of the $a_{cub.}$ parameter with increasing temperature was expected, because of the thermal dilatation of the unit cell. The curve highlights, on the contrary, a decrease in the cell parameter at the very beginning of the experience. Comparison of the curve of experimental points, obtained at RT (□), with the curve of experimental points, obtained at increasing temperature (■), shows clearly that two opposite effects occur simultaneously on the $a_{cub.}$ parameter, during the first part of the thermal treatment: an increase due to thermal dilatation and an intrinsic decrease due to a material modification. The cell parameter of a spinel phase is typically conditioned by the size of the octahedral B sites.[18] A contraction reveals therefore a decrease in the size of the octahedral cobalt site, which could be explained by the formation of Co^{4+} ions in octahedral sites.

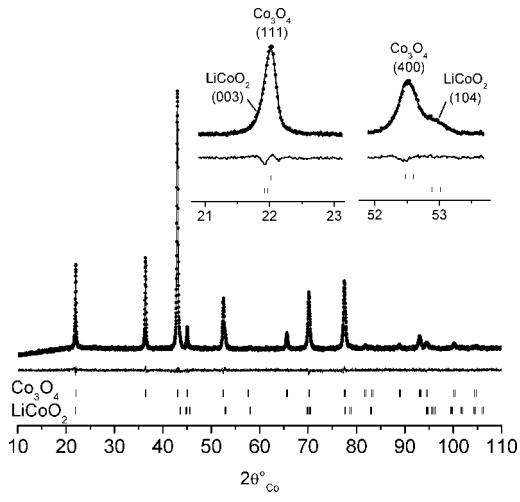

Figure 2. Comparison of the experimental (•) and calculated (−) X-ray powder diffraction patterns of the spinel-650 heat-treated sample. The difference between observed and calculated profiles and the diffraction lines positions (|) of the Co_3O_4 and $LiCoO_2$ phases are given. The zoom on the (111) and (400) lines, proposed in the inset, allows us to show the good quality of the refinement.

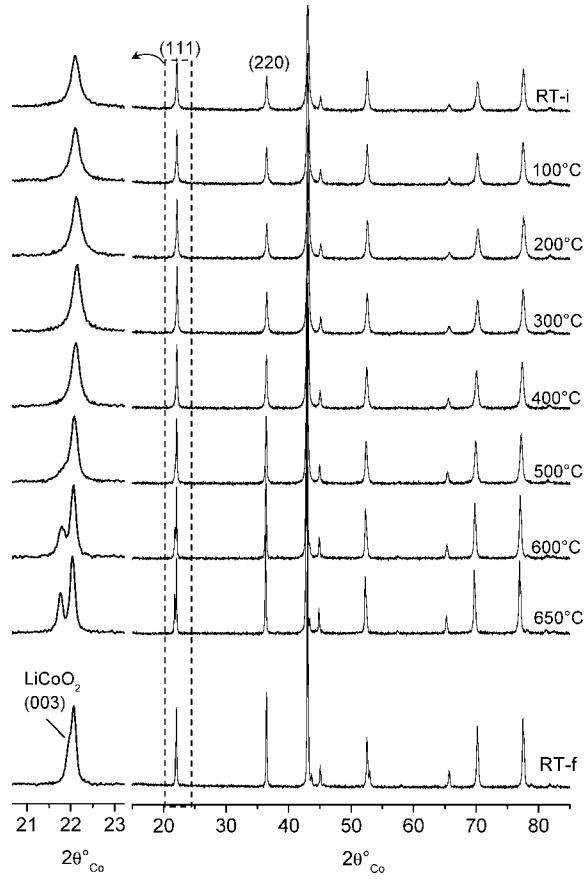

Figure 3. Evolution of the X-ray diffraction patterns with temperature, when heating the spinel-start material up to 650 °C, inside a variable-temperature chamber.

Table 3. Refinement Parameters of the XRD Patterns, Obtained during In situ Analysis of the Spinel-Start Sample (RT-i)

			cobalt occupancy		
acquisition *T* (°C)	$a_{cub.}$ (Å)	oxygen position "*u*"	8a sites	16d sites	wt % $LiCoO_2$
RT-i	8.0824(7)	0.2619(4)	0.77(2)	0.96(2)	
100	8.0849(4)	0.2618(4)	0.81(2)	0.98(2)	
200	8.0789(4)	0.2611(4)	0.78(2)	0.98(2)	
300	8.0880(4)	0.2616(4)	0.79(2)	0.98(2)	
400	8.1031(3)	0.2627(3)	0.87(2)	0.99(2)	
500	8.1173(5)	0.2631(3)	0.889(6)	0.97(2)	3.4(2)
600	8.1305(2)	0.2629(3)	0.93(2)	0.98(2)	7.2(3)
650	8.1389(2)	0.2622(3)	0.95(2)	0.98(2)	7.7(3)
RT-f	8.0813(2)	0.2632(3)	0.96(2)	0.99(2)	8.1(3)

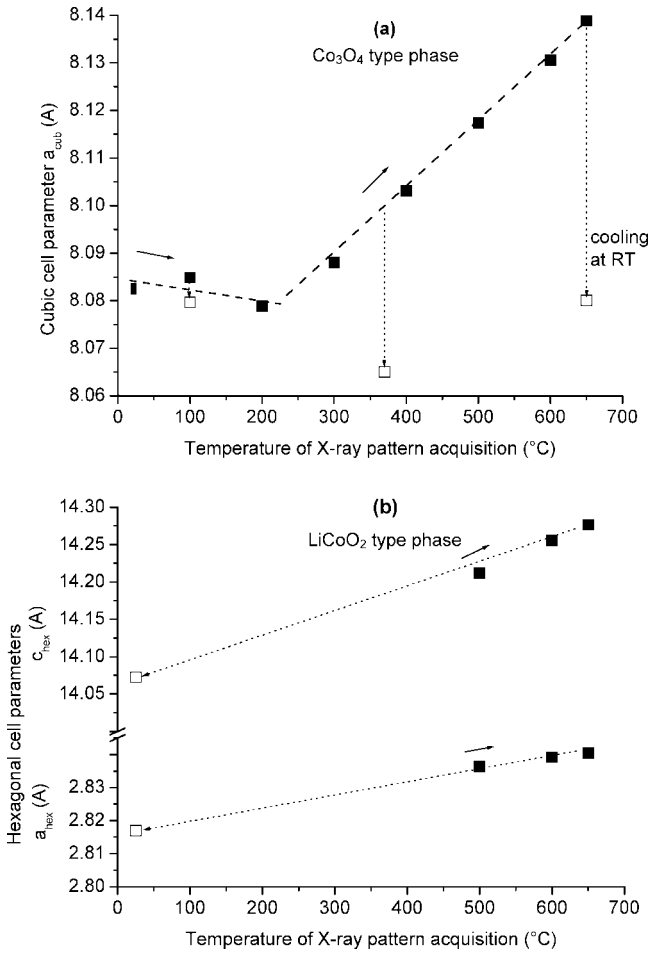

Figure 4. Variation of the cell parameter of (a) the spinel phase and (b) the $LiCoO_2$ type phase, with temperature increasing up to 650 °C, inside a variable-temperature chamber (■). The values, obtained for the heat-treated materials cooled at room temperature, are also displayed (□).

The $LiCoO_2$ phase progressively crystallizes, beyond 500 °C, in an irreversible way. The amount is evaluated to 8.1 wt % in the in situ experiment (Table 3), which is in agreement with the quantity calculated in the ex situ analysis (6.7 wt %, Table 3). Figure 4b shows that, contrarily to the case of the spinel phase, the cell parameters of the hexagonal phase exhibit a linear variation with temperature, due to thermal dilatation. Such variation supports the fact that the decrease of the $a_{cub.}$ parameter of the spinel phase is correlated to structural transformations.

The "*u*" parameter, which defines the relative oxygen position within the structure, is increased after heat treatment, and especially beyond 300 °C (see Table 3). This parameter can be a quantitative measurement of the distortion of the cubic close-packed arrangement of oxygen atoms. Indeed, in the AB_2O_4 spinel structure, depending on the relative sizes of the cations, the oxygen ions may move slightly to be closer to the A or B cation position, with cooperative contraction of the tetrahedral A sites and expansion of the octahedral B sites, or vice versa. A "*u*" value of 0.2625 corresponds to equal tetrahedral and octahedral Co−O bond lengths.[18] For ideal Co_3O_4, the "*u*" value is usually equal to 0.2631,[14,19] in accordance with the difference of ionic radius between Co^{2+} ions, in tetrahedral site, and Co^{3+} ions, in octahedral site. A lower "*u*" value, as for the "spinel-start" material (u = 0.2619), results from lower tetrahedral (1.916 Å) and higher octahedral (1.929 Å) Co−O bond lengths. The distortion that is observed for the "spinel-start" material, as compared with the ideal Co_3O_4 structure, is illustrated in Figure 5. This effect can be due to the presence of lithium and hydrogen ions, as well as of cationic vacancies, within the structure, which induces a displacement of the oxygen atoms. After heat-treatment, the "*u*" parameter for the material increases up to 0.2632 and gets closer to the value expected for an ideal spinel phase.

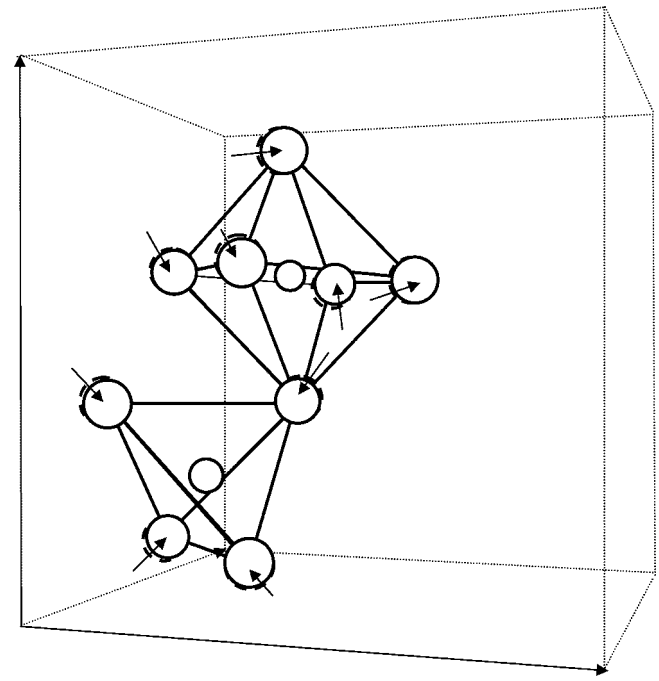

Figure 5. Schematic representation of the distortion of the cubic close-packed arrangement of the oxygen atoms, in a spinel structure, when the value of the u parameter decreases from 0.2631 (ideal Co_3O_4, represented by dashed circles) down to 0.2619 (represented by solid circles).

The thermal evolution of the cobalt occupancies within the spinel structure is represented in Figure 6. As shown by the general trend, temperature induces key modifications on the cobalt occupancy in 8a tetrahedral sites. In the starting material, only 77% of the tetrahedral sites are occupied by cobalt ions, whereas octahedral sites are almost filled. Beyond 350 °C, the cobalt occupancy in the tetrahedral sites increases with temperature, whereas it remains stable in octahedral sites. Thus, the atomic cobalt/oxygen ratio progressively increases, up to 0.735 (the theoretical ratio in ideal $Co[Co_2]O_4$ is equal to 0.75). The increase in the Co/O ratio implies a loss of oxygen atoms from the spinel structure. As will be discussed in the next sections (^{7}Li NMR and thermal analysis sections), water is continuously removed and LiOH is formed during the thermal treatment. The formation of H_2O, as well as of LiOH and $LiCoO_2$ in the final part of the thermal treatment, leads to an increase in the Co/O ratio in the spinel phase, thanks to a global reorganization.

(18) Hill, R. J.; Craig, J. R.; Gibbs, G. V. *Phys. Chem. Miner.* **1979**, *4* (4), 317–339.

(19) Roth, W. L. *J. Phys. Chem. Solids* **1963**, *25* (1), 1–10.

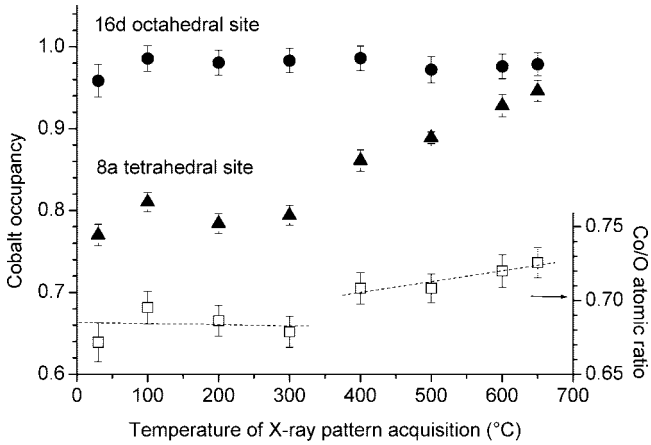

Figure 6. Variation of cobalt occupancy in the 8a tetrahedral sites (97>) and in the 16d octahedral sites (•), on the left Y-axis, and variation of Co/O atomic ratio (□), on the right Y-axis. The cobalt occupancies and the Co/O atomic ratio were determined by Rietveld refinement of the X-ray diffraction data (Table 3), collected for the spinel-start sample heated up to 650 °C, inside a variable-temperature chamber.

^{7}Li NMR. ^{7}Li NMR measurements were performed on the spinel-start material and on the spinel-370 and spinel-650 heat-treated samples; the spectra are shown in Figure 7. On the basis of the X-ray diffraction experiments, the initial material and the sample that was heat-treated at 370 °C appear to be monophasic, whereas the sample heat-treated at 650 °C contains 7 wt % $LiCoO_2$ type phase, in addition to the spinel phase.

The $Li_{1.0}CoO_2$ stoichiometric phase is an insulator, which results from the presence of Co^{III} diamagnetic ions (t_{2g}^6). Because of the ionic character of the Li−Co bond, lithium deintercalation occurs without structural modification of the host structure.[20] The electronic conductivity of the Li_xCoO_2 phase is strongly dependent on the lithium amount. Previous reports have clearly demonstrated, by electrochemical lithium extraction from $Li_{1.0}CoO_2$, the existence of a Li_xCoO_2 solid solution for $0.94 < x < 1.0$ and of a two-phase domain for $0.75 < x < 0.94$.[21] Moreover, electronic conductivity measurements have evidenced an insulator−metal transition during lithium deintercalation.[22] The lithium-rich solid solution exhibits a semiconductive behavior due to the Co^{3+}/Co^{4+} electron hopping, whereas Li_xCoO_2 with $x \leq 0.75$ exhibits a metallic character. Within the $0.94 < x < 1.0$ solid solution, the electronic conductivity changes by several orders of magnitude, whereas there is no significant change in the cell parameters. A way to differentiate the various lithium phases is NMR analysis: Li_xCoO_2 phases with $0.94 \leq x \leq 1.0$ exhibit indeed a single narrow signal at - 0.5 ppm; only a decrease of the intensity and of the T1 relaxation time of the signal is observed with lithium extraction. Indeed, the relaxation time of the NMR signal is very sensitive to the presence of paramagnetic species (as Co^{4+} ions), which shortens it drastically. When $0.94 < x \leq 0.75$ (two-phase domain), a new Knight-shifted signal appears at 57 ppm,

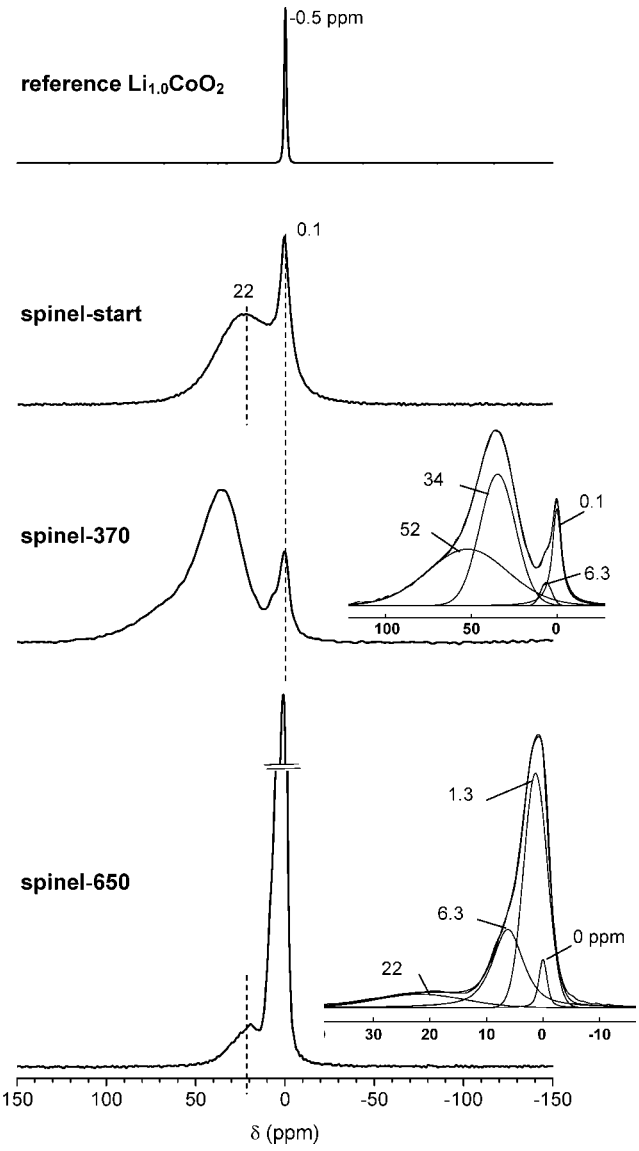

Figure 7. ^{7}Li MAS NMR spectra of the samples, starting and heat-treated at 370 and 650 °C, in comparison with stoichiometric $Li_{1.0}CoO_2$, obtained by classical solid-state reaction. The spectra of the three materials are plotted in a common absolute intensity scale.

whereas for $x < 0.75$, the signal at −0.5 ppm disappears, whereas the signal at 57 ppm shifts further.[22]

Two different signals at 0.1 and 22 ppm are observed in the starting material (spinel-start), in Figure 7. The 22 ppm signal is assigned to lithium in the metallic-like spinel structure,[8] whereas the narrow signal, which has a T1 relaxation time higher than 4 s, is attributed to Li_2CO_3 in the material. This latter signal corresponds to around 25% of the lithium atoms in the material, i.e., around 3 wt % lithium carbonate (considering the total amount of Li determined by ICP analysis mentioned below), which can therefore not be detected by X-ray diffraction.

The spectrum of the spinel-370 heat-treated sample exhibits four distinct signals at 0.1, 6.3, 34, and 52 ppm. The 0.1 ppm signal is assigned to Li_2CO_3, which is known to be stable for temperatures up to 750 °C. The two signals at 34 and 52 ppm can be correlated to two new lithium species within the spinel structure (as compared to the 22 ppm signal in the starting material, which has disappeared

(20) Orman, H. J.; Wiseman, P. J. *Acta. Crystallogr., Sect. C* **1984**, *40* (1), 12–14.
(21) Reimers, J. N.; Dahn, J. R. *J. Electrochem. Soc.* **1992**, *139* (8), 2091–2097.
(22) Ménétrier, M.; Saadoune, I.; Levasseur, S.; Delmas, C. *J. Mater. Chem.* **1999**, *9*, 1135.

here). The minor signal observed at 6.3 ppm is to date unexplained. With a relaxation time higher than 400 ms, it cannot be related to lithium within the metallic spinel phase, or to any known Li_xCoO_2 type-phase. A $Li_{1-x}Co_xO_2$ type phase,[23] formed by decomposition of the lithiated spinel-type phase, could explain this signal at 6.3 ppm. Such a phase is indeed detected by XRD, after a TGA experiment up to 850 °C.

The spectrum of the spinel-650 heat-treated sample exhibits four different signals: a signal at 0 ppm, a new and majority signal (63% of lithium in the material) close to 1.3 ppm and two secondary signals at 6.3 and 22 ppm. The 0 ppm signal is assigned to an overlap of the signals, corresponding to Li_2CO_3 and $LiCoO_2$, newly formed in the material in addition to the spinel phase. The T1 relaxation time is higher than 400 ms, which excludes the possibility of a Li_xCoO_2 phase, with a lithium content in the $0.94 < x < 1$ range, containing localized Co^{4+} ions.[22] Besides, x cannot be lower than 0.94, because no signal is observed at 57 ppm. Therefore, the lithium cobaltite phase present is the stoichiometric $Li_{1.0}CoO_2$ phase. The signal that appears at 22 ppm is assigned to lithium in spinel structure, as for the parent material. These changes between "spinel-370" and "spinel-650" highlight a migration of the lithium ions toward new sites and/or changes in the cobalt oxidation states within the spinel structure when the temperature increases. It is surprising to observe that the spinel phase changes with temperature and comes back to the initial state (22 ppm shift in "spinel-start" and in "spinel-650" materials). Let us note, however, that the magnitude of the signal corresponding to lithium in the spinel structure has drastically decreased in the heat-treated material, which may be correlated with the departure of lithium from the spinel structure. Finally, the majority signal, observed at 1.3 ppm, is very similar to that expected for LiOH (reference not shown here). This phase, which was not observed by XRD, could be in an amorphous form or as a thin surface layer.

Consequently, the lithium cobaltite phase that has grown during heat-treatment is unambiguously the $Li_{1.0}CoO_2$ insulating stoichiometric phase, which can not be responsible for the high conductivity of the final material. This result is in agreement with Kellerman et al., who have proved the thermal instability of nonstoichiometric $Li_{1-x}CoO_2$ lithium cobaltites [24], which are decomposed to stoichiometric $Li_{1.0}CoO_2$ phase at 600 K, according to the following reaction: $Li_{1-x}CoO_2 \rightarrow (1-x)Li_{1.0}CoO_2 + (x/3)Co_3O_4 + x/3O_2$. In addition, our NMR measurements highlight the changes within the spinel structure with the temperature increase, and the formation of a LiOH type phase, beside lithium cobaltite.

Thermal Analysis. The thermal behavior of the spinel-start sample was studied by thermogravimetric analysis, coupled with mass spectroscopy, under argon flux. Figure 8 presents (a) the TGA curve (full line) and its derivative curve (dotted line), as well as (b) mass spectroscopy curves of the main released species. MS analysis highlights two main phenomena: a quasi-continuous departure of H_2O and CO_2 gas, from room temperature to 700 °C, and a high release of O_2 beyond 700 °C. Below 100 °C, the small weight loss (0.38%) observed can be ascribed to the release of adsorbed surface water only. In the 100−700 °C range, the weight loss (3.49%) could be associated with a release of adsorbed surface water and a simultaneous decomposition of hydroxyl groups within the structure, with formation of water molecules. The CO_2 release is attributed to gas adsorbed on the surface of the material and will not be considered thereafter, because the amount of carbon, detected by ICP analysis in the material, was negligible. The strong weight loss (6.45%), observed beyond 700 °C, corresponds to the Co_3O_4-CoO transition, which indeed theoretically involves a 6.64% weight loss, corresponding to oxygen exhaust.

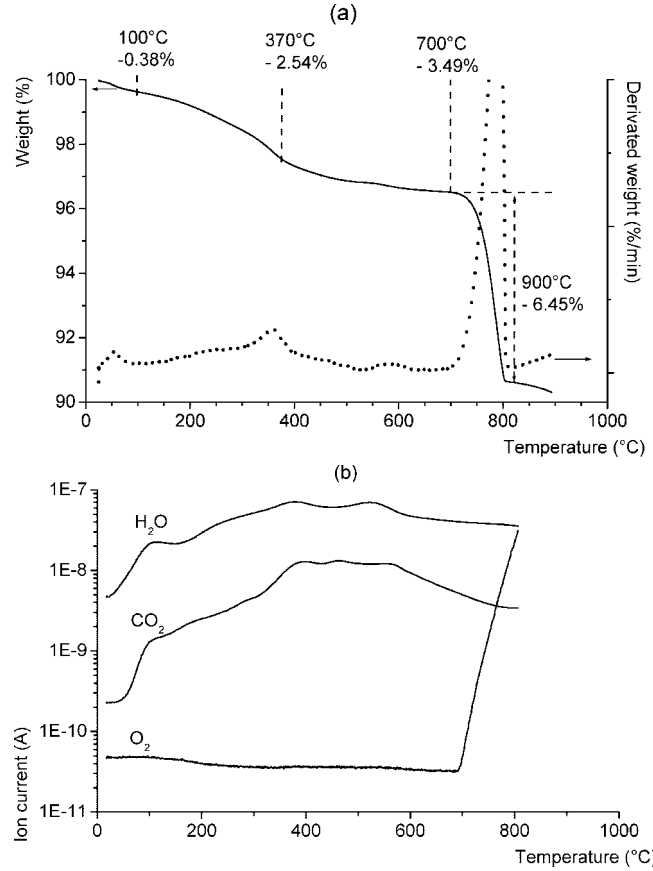

Figure 8. (a) TGA curve, with its derivative curve (dotted line), and (b) coupled mass spectroscopy curves, obtained for the spinel-start sample.

TGA measurements were also carried out from "spinel-start", under oxygen flux, and led to weight losses that are similar to those obtained under argon flux until 700 °C. Oxygen atmosphere has therefore no influence on the material evolution during the heat treatment, so that oxidation of the material by atmospheric oxygen can be excluded.

Chemical Composition. Chemical compositions of the starting material and of the heat-treated samples are summarized in Table 4, which presents the weight percentage of Co, Li, and H. With the CHNS analysis method, the accuracy of the measurement of hydrogen amounts, lower than 0.3%, is not sufficient. The hydrogen amounts in the four samples were therefore estimated on the basis of water

(23) Johnston, W. D.; Heikes, R. R.; Sestrich, D. *J. Phys. Chem. Solids* **1958**, *7*, 1–13.
(24) Kellerman, D. G.; Karelina, V. V.; Blinovskov; Y, N.; Gusev, A. I. *Russ. J. Inorg. Xhem.* **2002**, *47* (6), 884–890.

Table 4. Weight Percentages of Cobalt, Lithium, and Hydrogen; Corresponding Molar Ratio; and Average Oxidation State of Cobalt in the Spinel-Start Material and in the Heat-Treated Samples[a]

material	wt % Co	wt % Li	wt % H	H/Co atomic ratio	Li/Co atomic ratio	average oxidation state of Co
spinel-start	69.00	0.69	0.38	0.32	0.09	2.78
spinel-100	68.34	0.69	0.40*	0.34	0.09	2.79
spinel-370	69.42	0.69	0.19*	0.16	0.09	2.79
spinel-650	69.68	0.69	0.11*	0.09	0.09	2.76

[a] The weight percentages were determined by ICP titration, except for hydrogen in the heat-treated materials (*), which was deduced from TGA measurements.

losses observed by TGA, between room temperature and 700 °C (TGA curves are not presented here). Let us note that for the "spinel-100" sample, the two methods (TGA and CHNS) lead to the same value of 0.4 wt % hydrogen. The amounts of carbon and potassium were very low and will therefore be neglected.

The significant amount of hydrogen detected, especially in the spinel-start and spinel-100 materials, suggests that it can be located only at the surface of the particles, but also inside the spinel structure. According to litterature, in such spinel structures, the hydrogen atoms are likely to be located in 8a, 48f,[25] or 96g sites.[26,27] A proton NMR study is planned in order to try to localize them in the structure. The progressive decrease in the hydrogen amount during the successive three annealings is in agreement with the continuous release of H_2O, shown by mass spectroscopy. As far as the Li/Co ratio is concerned, it remains constant and equal to 0.09, whatever the temperature. The presence of a significant amount of lithium is in accordance with the existence of a mixed Li−Co spinel phase, as claimed in the X-ray analysis section. The formation of 7 wt % $LiCoO_2$ in the heat-treated spinel-650 material suggests that a significant amount of lithium ions is still present in the spinel structure.

The average oxidation state of cobalt, measured by iodometric titration, is almost identical in the four samples, whatever the thermal treatment. The value is higher than that expected in an ideal $Co^{II}Co^{III}{}_2O_4$ spinel phase (2.66) and confirms therefore the presence of Co^{IV} in the structure. If one considers that no redox process occurs with the external atmosphere during thermal treatment, as deduced from TGA measurements, H_2O and LiOH releases do not modify the average oxidation state of cobalt in the spinel phase. Nevertheless, the formation of a small amount of $LiCoO_2$ in the spinel-650 sample tends to a very slightly lower oxidation state of cobalt in the spinel phase at this temperature.

Electrical Properties. Electronic conductivity measurements of the starting material were performed in the −100 to 400 °C range, in an argon or oxygen atmosphere, and led to similar behaviors in both cases. The variation of conductivity logarithm versus reciprocal temperature is presented in Figure 9. The curve shows a significant increase in the conductivity of the material with temperature.

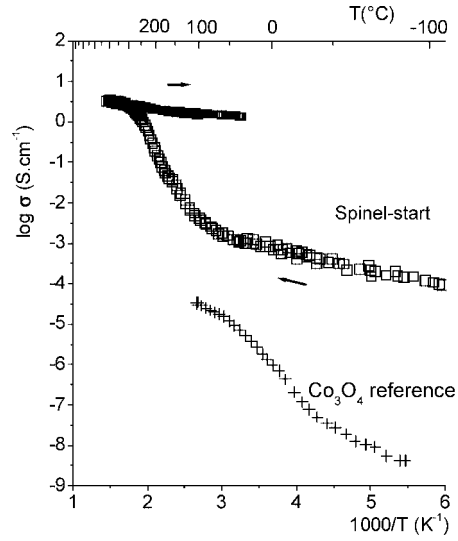

Figure 9. Variation of logarithm of electrical conductivity versus reciprocal temperature, for the starting material, in comparison with reference Co_3O_4, obtained by classical solid-state reaction.

The starting material exhibits an electronic conductivity ($\sigma_{RT} = 1.6 \times 10^{-3}$ S cm^{-1}, activation energy $E_a = 0.12$ eV) that is considerably higher than that of classical Co_3O_4 ($\sigma_{RT} = 5 \times 10^{-6}$ S cm^{-1}). The presence of Co^{4+} ions in the octahedral site subnetwork leads to a partially filled (Co^{3+}/Co^{4+}) t_{2g} band, leading to a tendency to delocalize the electrons. Nevertheless, the small amount of Co^{4+} and the presence of defects such as cobalt vacancies and H^+ or Li^+ ions in the structure restricts the electronic delocalization to the local scale.

During heating, the curve shows until 430 °C a strong irreversible increase in the electronic conductivity of the material. At the end, the room-temperature electronic conductivity has increased by 3 orders of magnitude ($\sigma_{RT} = 1.5$ S cm^{-1}, $E_a = 0.03$ eV). This evolution is in agreement with the increasing amount of Co^{4+} ions in octahedral sites, which occurs during the thermal treatment, as previously discussed. As the $LiCoO_2$ phase is formed beyond 500 °C only, it cannot be responsible for the high conductivity of the material. Therefore, the observed increase in conductivity results from the change in composition of the spinel phase. Nevertheless, a small contribution of the particle size, which increases and therefore tends to lower the number of grain boundaries, cannot be totally excluded.

General Discussion. In a previous study, we have shown that the electrochemical synthesis of a cobalt spinel derivative, in a mixture of LiOH, NaOH, and KOH, leads to a material with an electronic conductivity much higher than that of classical Co_3O_4. In this material, the presence of cobalt vacancies and Li^+ ions in the tetrahedral sites leads, for charge compensation, to the formation of Co^{4+} ions in the $[Co_2O_4]$ octahedral framework, which allows an electronic delocalization at the local scale. The presence of a very large number of defects prevents the formation of a metallic phase.

In this paper, one tries to understand what is going on during the heat-treatment of this material in order to relate the conductivity changes to structural modifications. From the experimental work reported in this paper, the following results must be considered:

(25) Kelder, E. M.; Simon, R.; Wagemaker, M.; Mulder, F. M.; Schoonman, J. *Solid State Ionics* **2006**, *177* (26−32), 2759–68.
(26) Ammundsen, B.; Jones, D. J.; Rozière, J.; Berg, H.; Tellgren, R.; Thomas, J. O. *Chem. Mater.* **1998**, *10* (6), 1680–1687.
(27) Aitchison, P.; Ammundsen, B.; Bell, T.; Jones, D.; Roziere, J.; Burns, G.; Berg, H.; Tellgren, R.; Thomas, J. *Physica B* **2000**, *276*, 847–848.

The thermal treatment at 430 °C leads to an irreversible increase in conductivity by 3 orders of magnitude.

H_2O is removed from the material in two steps. The first one, below 120 °C, corresponds to absorbed water; the second one occurs with increasing temperature, with two maxima at 350 and 550 °C.

$LiCoO_2$ appears beyond 500 °C. Therefore, this phase does not contribute to the increase in conductivity.

A LiOH type phase (traces detected by NMR) emerges in the final part of the heat-treatment.

The thermal variation of the unit-cell parameter of the spinel phase results from the competition between the dilatation effect and an intrinsic decrease, which occurs mainly in the intermediate temperature range (150−400 °C).

A significant increase in the Co/O atomic ratio in the spinel phase is observed above 350 °C.

The amount of cobalt in the octahedral sites of the spinel phase is nearly constant.

The amount of cobalt in the tetrahedral sites of the spinel phase increases also above 350 °C.

The average oxidation state of cobalt is not significantly modified all along the thermal treatment.

On the basis of the X-ray structural refinement results (percentage of cobalt in the tetrahedral and octahedral sites and Co/O ratio) and of the cobalt oxidation state (2.78), formulations can be proposed as follows:

$H_xLi_yCo^{II}_{0.77}[Co^{III}_{1.74}Co^{IV}_{0.18}]O_4$ for the spinel-start starting material at room temperature.

$H_{x'}Li_{y'}Co^{II}_{0.82}\ [Co^{III}_{1.65}Co^{IV}_{0.23}]O_{3.79}$ for the material obtained at 400 °C during the in situ analysis. The latter formulation supposes the presence of oxygen vacancies within the spinel structure. Nevertheless, at high temperature, vacancies could migrate from the bulk to the material surface thanks to thermal energy, leading to a contraction of the structure. In this case, the resulting formula can be written as: $H_{x''}Li_{y''}Co^{II}_{0.87}\ [Co^{III}_{1.74}Co^{IV}_{0.24}]O_4$. The hydrogen and lithium amounts in the spinel structure are intentionally not specified in the above formulas, because of the unquantified presence of adsorbed water and lithium carbonate in the material. Nevertheless, these formulas clearly show the overall transfer of cobalt from octahedral toward tetrahedral sites and the increase of the amount of Co^{IV} atoms with temperature. The departure of hydrogen should be the driving force of this cationic migration.

The following mechanism can be proposed on the basis of all these results: the protons are no longer stable within the structure at increasing temperature. Their removing, as H_2O molecules, requires partial reorganization of the spinel structure (O−H and O−Co bond breaking), leading to an increase of the Co/O atomic ratio in the spinel phase. A very similar structural reorganization was observed during the deintercalation of lithium for the $Li_{1+x}(Mn_{0.425}Ni_{0.425}Co_{0.15})_{1-x}O_2$ phase.[28] In the latter material, at the very end of the deintercalation, when all cations are at the tetravalent state, it is possible to extract electrochemically more Li^+ ions. In fact, Li^+, electrons and oxygen ions are then simultaneously extracted from the material. It follows that Li_2O is removed at room temperature from the material, through a structural reorganization, which increases the M/O atomic ratio (M = Ni, Co, Mn) and does not affect the crystallinity of the material. By analogy, in our material, Li_2O could be removed from the spinel to form, with H_2O, a LiOH phase. In this case, the reaction is easy, because it occurs at high temperature.

As the spinel framework is built up from edge-sharing CoO_6 octahedra, the filling of the octahedral sites is maintained in first approximation, as confirmed by XRD. As a result of the increase of the Co/O ratio, the amount of cobalt in tetrahedral sites slightly increases. Furthermore, the global oxidation state of cobalt does not change. From crystal field considerations, only Co^{2+} ions are stable in tetrahedral site. Therefore, there is an increase of the Co^{4+}/Co^{3+} ratio in the $[Co_2O_4]$ octahedra framework, and consequently an increase of the conductivity by 3 orders of magnitude. Moreover, the activation energy decreases significantly ($\Delta E = 0.12$ eV for the starting material and $\Delta E = 0.03$ eV after heating at 400 °C). We can assume that the thermal treatment, which reduces the amount of hydrogen and the number of cobalt vacancies in tetrahedral sites, also makes the electronic delocalization easier, thanks to the removal of a large number of defects that tend to localize the electrons.

Conclusion

This study was focused on the thermal behavior of a highly conductive $H_xLi_yCo_{3-\delta}O_4$ spinel phase, synthesized by electrochemical oxidation of CoO powder, and which can be used as conductive additive in Ni-MH batteries. Modifications occurring in the structure of the material during a heat-treatment were investigated. In-situ XRD analysis shows that the departure of H_2O, the increasing Co/O atomic ratio, the increasing amount of Co^{2+} in tetrahedral sites and the jump in electronic conductivity, occur simultaneously around 350 °C. The increase in the Co^{4+}/Co^{3+} ratio in the $[Co_2O_4]$ octahedral framework and the removing of a large number of defects entails the increase of the electronic conductivity by 3 orders of magnitude.

Acknowledgment. The authors are very grateful to Laurence Croguennec for fruitful disscussions concerning the structural determinations of the materials. The authors wish to thank C. Denage and P. Dagault for technical assistance, E. Lebraud and S. Pechev for X-ray diffraction, R. Decourt for electric properties measurements, D. Denux for mass spectroscopy analysis, and E. Suard (ILL) for neutron diffraction data collection. SAFT, ANRT, and Region Aquitaine are acknowledged for their financial support.

CM801775G

(28) Tran, N.; Croguennec, L.; Menetrier, M.; Weill, F.; Biensan, P.; Jordy, C.; Delmas, C. *Chem. Mater.* **2008**, in press.